Prot. n. 194 del 20 giugno 2005

IPCF Rapporto Interno N. 2/200605

R&D ON BRIGHT, ULTRAFAST X-RAY SOURCES DRIVEN BY INTENSE FEMTOSECOND LASER PULSES

Leonida A. GIZZI, Marco GALIMBERTI, Antonio GIULIETTI, Danilo GIULIETTI, Petra KOESTER, Luca LABATE, Paolo TOMASSINI

Abstract. This report describes the study of X-ray emission from ultra-fast laser interactions with solids presently in progress at the Intense Laser Irradiation Laboratory. We describe the dedicated equipment including a powerful femtosecond, Titanium-Sapphire laser system and custom developed diagnostics for the characterization of both the laser performance and the X-ray emission. We show the first experimental results obtained from irradiation of Aluminium and Titanium targets that demonstrate the operational conditions of our ultrafast X-ray source. X-ray spectra obtained from these materials and analysed by single-photon counting and spectroscopy provide direct evaluation of peak and average X-ray photon fluxes achievable with our source.

Laboratorio per l'Irraggiamento con Laser Intensi
ISTITUTO PER I PROCESSI CHIMICO-FISICI
Area della Ricerca CNR, Via Moruzzi, 1 56124 Pisa, Italy - http://ilil.ipcf.cnr.it
e-mail l.a.gizzi@ipcf.cnr.it

R&D ON BRIGHT, ULTRAFAST X-RAY SOURCES DRIVEN BY INTENSE FEMTOSECOND LASER PULSES

Leonida A. GIZZI, Marco GALIMBERTI, Antonio GIULIETTI, Danilo GIULIETTI,
Petra KOESTER, Luca LABATE, Paolo TOMASSINI

Intense Laser Irradiation Laboratory, ISTITUTO PER I PROCESSI CHIMICO-FISICI
Area della Ricerca CNR, Via Moruzzi, 1 56124 Pisa, Italy - *http://ilil.ipcf.cnr.it*

1.Introduction

Laser-plasmas are well-known for their X-ray emission properties and X-ray sources based on such plasmas are routinely used for a wide range of applications in which high peak power and moderate average power X-ray sources are required [1]. More recently, the development of high repetition rate, powerful femtosecond laser systems is making widely available a new generation of laser-driven X-ray sources characterised by a very short pulse duration, well below the pulse duration of synchrotron radiation pulses and comparable with the pulse duration of future fourth generation, LINAC based, X-ray Free Electron Lasers (XFEL).

The interaction of focused, intense CPA (Chirped Pulse Amplification) [2] laser pulses with a solid targets produces "hot" electrons that penetrate in the cold target substrate and generate incoherent X-ray emission due to K-shell transitions. Currently, sources based on this effect provide a unique approach [3] to femtosecond, X-ray probing of matter for the understanding of ultrafast phenomena [4] such as the recently demonstrated non-thermal melting of semiconductors [5]. In this report we describe the activity ongoing in this field at the Intense Laser Irradiation Laboratory of IPCF-CNR in Pisa. This activity is partially supported by the national programme on "Novel X-ray sources for multidisciplinary applications" funded by the Italian Ministry of Education and Research.

2. Background

The primary process for ultra-fast X-ray emission from intense CPA laser irradiation of solids is the generation of longitudinal electrostatic plasma waves. Resonance absorption of the laser light at the critical density is a possible source mechanism for this generation [6]. In fact, due to the short pulse-length, a steep plasma density gradient is established early during the interaction. In the case of *p*-polarised laser radiation, efficient energy transfer of laser energy to the plasma can occur [7], giving rise to longitudinal electrostatic electron plasma waves. The subsequent damping of the electron plasma wave, occurring through collisionless damping processes, leads to the generation of a population of hot electrons, having a temperature of tens to hundreds of keV.

As shown in Figure 1, energetic electrons produced in the plasma can penetrate into the underlying colder material. Here, they knock out electrons preferentially from the inner electronic shell of the atoms, thus producing core holes. The radiative transitions of electrons from the outer shells finally leads to the generation of characteristic K lines.

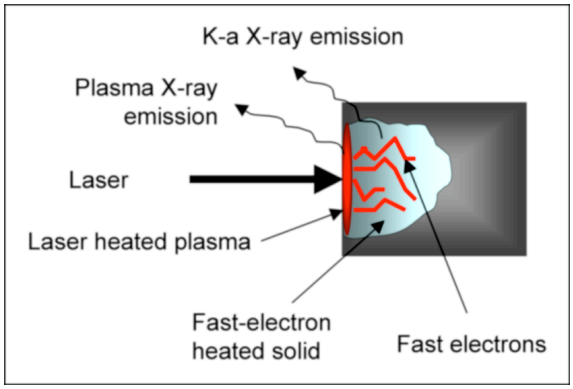

Figure 1. Diagram showing the basic mechanisms of K-alpha X-ray generation from ultrafast, intense laser interaction with solid targets.

This process is particularly efficient in the case of short pulse irradiation because of the efficiency of the electron plasma wave generation process [8,9]. This is the reason why these sources are growingly used for novel applications.

X-ray sources based upon this process are characterized by duration and size comparable respectively to the laser pulse duration and spot size [10]. This is significantly different from laser-plasma sources based upon picosecond and nanosecond laser pulses where the X-ray emitting region is basically determined by the hydrodynamic expansion of the plasma [1]. Therefore, in order to control the temporal and spatial properties of the X-ray source, a detailed knowledge of laser pulse parameters are required, including pulse energy and duration, and intensity distribution in the interaction region. Information is also needed concerning the pre-pulse intensity, as well as the ps and ns contrast ratio. In fact, precursor laser radiation may lead to a premature plasma formation that is well known to affect the plasma properties at the time of interaction of the main pulse [11] . In view of this, several measurements were carried out on the fs laser systems used at ILIL. A detailed description of these measurements is given in the following paragraph.

2. The femtosecond laser source

The R&D on ultra-short, higher photon energy sources is based on a new Ti:Sa system delivering <80 fs pulses with peak power exceeding 120 GW, at the repetition rate of 10 Hz. A schematic view of the entire system is shown in Figure 2. A picture of the actual system is given in Figure 3.

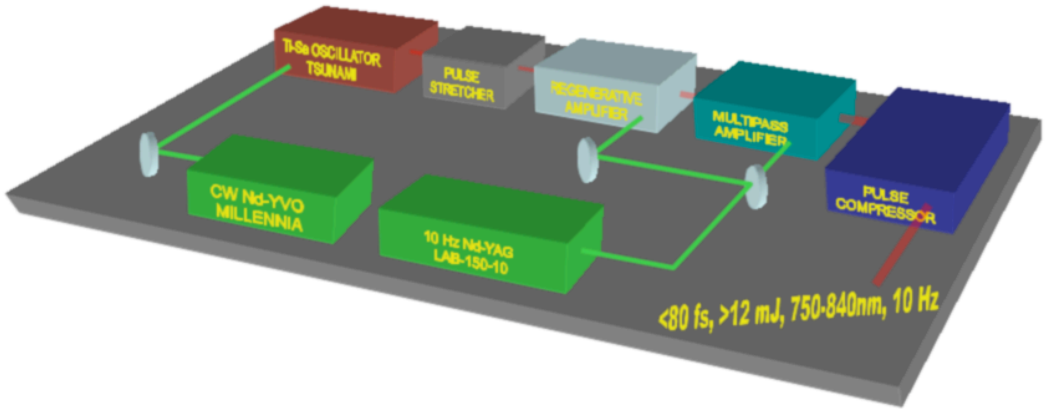

Figure 2. Schematic diagram of the high-power, femtosecond laser system used at ILIL-IPCF for the R&D activity on ultra-fast X-ray sources.

A femtosecond oscillator, a Tsunami (Spectra Physics), pumped by a diode-pumped 5W Nd:YVO, generates sub 50 fs pulses that are stretched and seeded into a regenerative amplifier.

The regen. amplifier is pumped by a fraction of frequency doubled, Nd:YAG, Q-switched laser pulses at a 10 Hz repetition rate. After amplification at the 2 mJ level, the stretched pulses are further amplified by a two-pass amplifier pumped by the remaining fraction of the Nd:YAG pulses. The output stretched pulses, containing an energy of approximately 18 mJ, are then compressed again to the fs pulse duration.

The temporal and spatial properties of the femtosecond pulses have been characterised in detail using custom developed devices. The temporal profile of the pulse was measured with a second order auto-correlator based on the set-up shown in Figure 4. The full power pulse, attenuated by three reflections off high quality uncoated glass flats ($\approx 10^5$ attenuation), is spit in two equally intense pulses using a beam splitter. One of the pulses is sent through an optical delay line. Both pulses are then focused on a 100 µm thick BBO crystal using a 5 cm focal length doublet. As shown in Figure 4, the two beams are set to impinge on the crystal with an angle of incidence of approximately 3 deg. As displayed by the small picture inside Figure 4 (left), the auto-correlation second harmonic (SH) radiation is emitted along the normal to the target while self-generated SH is collinear with the incident pulses. In this configuration, SH auto-correlation signal is detected in the forward direction while self-generated SH emission of each pulse can be discarded by a simple angular selection.

Figure 3. Picture showing the two-stage amplifier of the TiSa laser system at ILIL. Also shown in the background is the Tsunami fs oscillator (right) and the Nd:YAG pump laser (top-left).

The autocorrelation curve obtained from a scan of the delay of approximately 1 ps around the maximum SH signal is shown in Figure 4 (right). The data points fitted with a double Gaussian function, to take into account the low intensity tails of the curve, yield a FWHM of 67 fs.

The spatial quality of the laser pulse has also been studied by means of an equivalent plane monitor (EPM) based on a 100 cm nominal focal length optics and a 12 bits CCD camera (a Photometrics *Sensys*) with a pixel size of 8 µm edge. Figure 5 shows an image of the beam taken with the EPM at a distance of 7.5 cm before the best focus of the 100 cm optics. The plot on the right shows a lineout of the beam image fitted with a Gaussian curve. The plot of Figure 6 shows the FWHM of the focused laser spot versus distance, for the 1 meter focal length lens. A fit for this quantity using the function for a Gaussian beam is also shown.

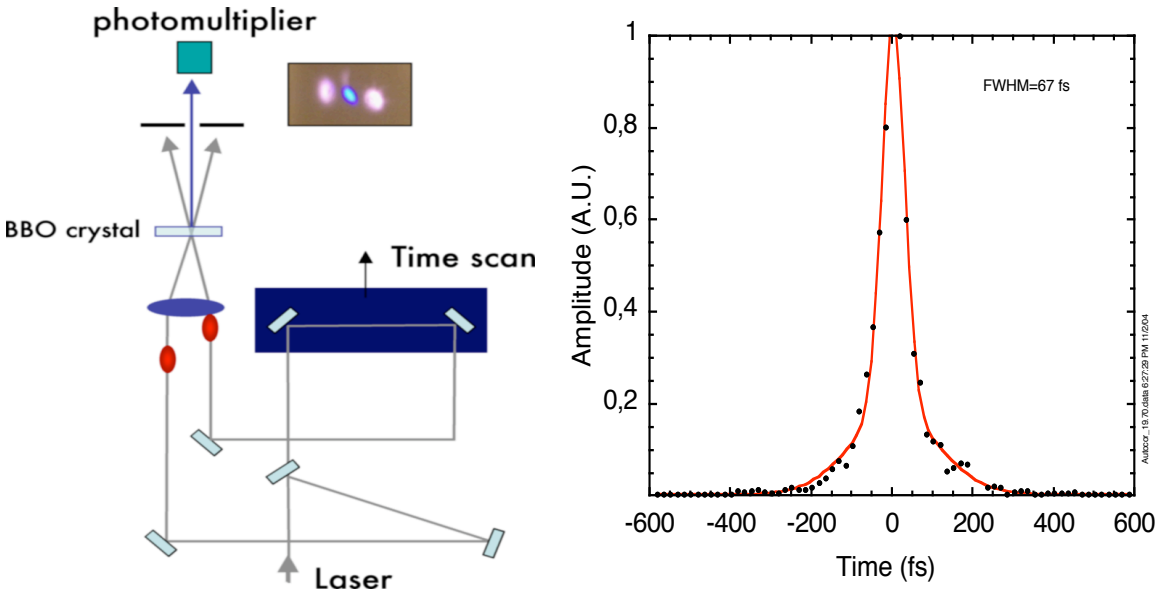

Figure 4. (Left) Schematic diagram of the second order auto-correlator used for the measurement of the laser pulse generated by the ILIL femtosecond laser system. The image taken after the focus shows the two infrared beams and the blue beam in the middle, as obtained with a diffused screen. (Right) Autocorrelation trace of the laser pulse at full amplification. The trace was fitted with a double Gaussian function to account for the real pulse shape.

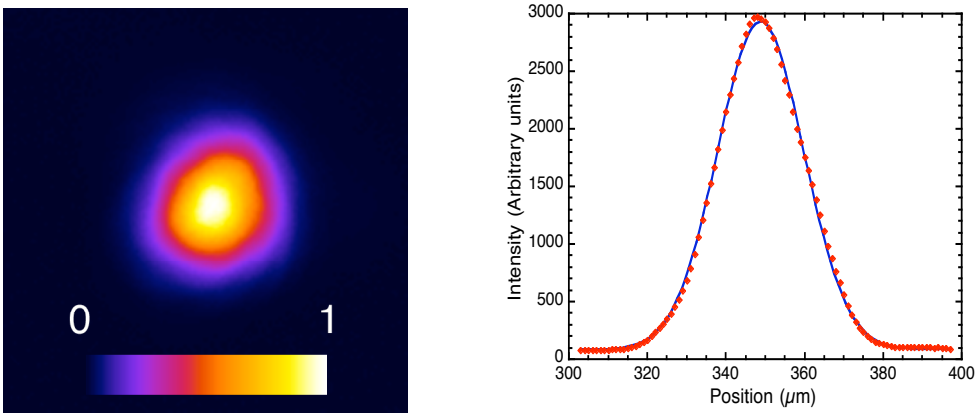

Figure 5. (left) Equivalent plane imaging of the laser beam taken at a distance of 7.5 cm before the nominal focal position of a 100 cm focal length. (right) Horizontal lineout (taken along the diameter) of the beam image on the left. The solid line (blue in the color version), shows the best fit obtained with a Gaussian function.

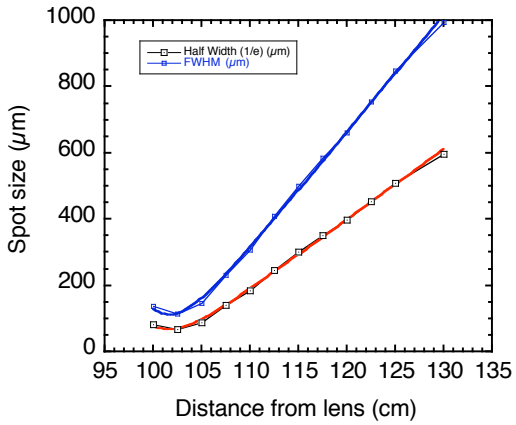

Figure 6. FWHM of the laser beam as retrieved at different distances from a 100cm nominal focal length lens. A fit with the function for a gaussian beam is also shown.

Both the temporal and spatial data show a high quality femtosecond pulse, focusable in a spot size very close to the diffraction limit. According to this result, the FWHM of the pulse best focus for the 100 cm optics is approximately 100 µm.

Scaling this value to the 10 cm focal length typically used in our experiments, we can assume a FWHM focal spot of approx. 11 µm. Considering the pulselength of 67 fs and an energy of 15 mJ we find that the peak intensity on the targhet can exceed 10^{17} W/cm^2.

2. Preliminary measurements

A preliminary source characterisation campaign has been performed at ILIL to identify the best set of experimental parameters for an efficient generation of ultra-short X-ray pulses. Basic diagnostic devices were adopted for the detection and measurement of primary parameters of X-ray bursts produced in the experiment. The fs laser pulse was focused on target using a 10 cm focal length optics. Either cylindrical targets of foil targets were used in our experiments. Helicoidally rotation or x-y translation were used respectively to ensure series of multi shot measurements.

As shown in the experimental set-up drawn schematically in Figure 7 The spectra of the X-rays generated by the interaction were measured using two types of detectors. One was based upon flat and bent crystals arranged in a first order Bragg configuration [12, 13, 14] for the characterization of spectral properties. This technique was aimed at achieving high resolution spectra capable of resolving the contribution to the total emission of X-rays of various transitions (K-alpha, K-beta etc.).

In addition, a spectroscopic technique based on the direct use of a cooled CCD detector (Princeton Intruments) in single photon mode [15] was used. This detection technique enables a simultaneous measurement of spectral properties and incident flux of the X-rays. In contrast with the measurement based upon Bragg crystals, this technique allows a reliable estimate of the X-ray photon yield to be made without independent calibration. One important issue to be tackled in this class of experiments with high intensity laser pulses is the noise arising from fast electrons produced by the interaction and escaping from the target. To this purpose it is interesting to compare the spectra obtained using the same spectrometer, equipped with a cooled CCD detector, irradiating a solid Al target with a nanosecond, low focused intensity laser pulse and with a relatively high focused intensity obtained with a CPA pulse.

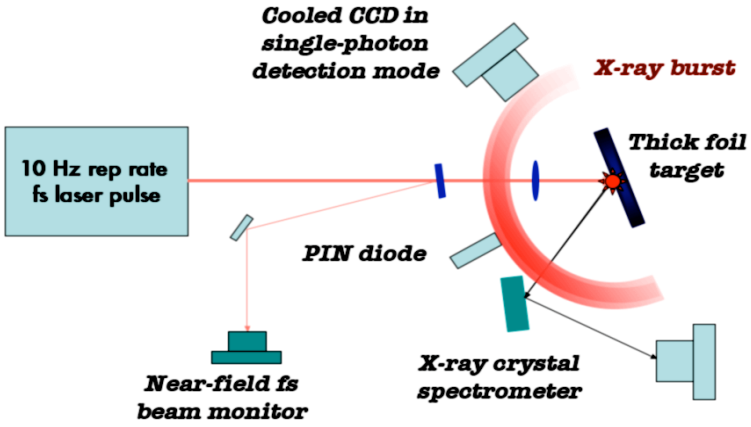

Figure 7. Schematic view of the experimental set up for the generation and detection of short pulse X-ray radiation from intense laser-solid interaction. The gradient-filled circular sector represents schematically the burst of X-rays originating from the target and emerging only from the front side of the target, emission from the rear-side being absorbed as in the case of very thick target substrate.

As displayed by the raw spectral images of Figure 8 the spectrum on the left shows the He-alpha line from He-like Al. When irradiating the sample with a higher focused intensity, short

pulse laser, another X-ray line appears on the low energy side of the He-alpha, namely the Al K-alpha line. Also visible in the same raw image is the noise consisting of few-pixel events uniformly distributed across the image. These randomly distributed events are due either to hard X-ray photons generated by bremmstrahlung of energetic electrons escaping from the target and impinging on equipment inside the target chamber (e.g. the crystal and/or the crystal holder), or by direct interaction of these electrons with the CCD chip.

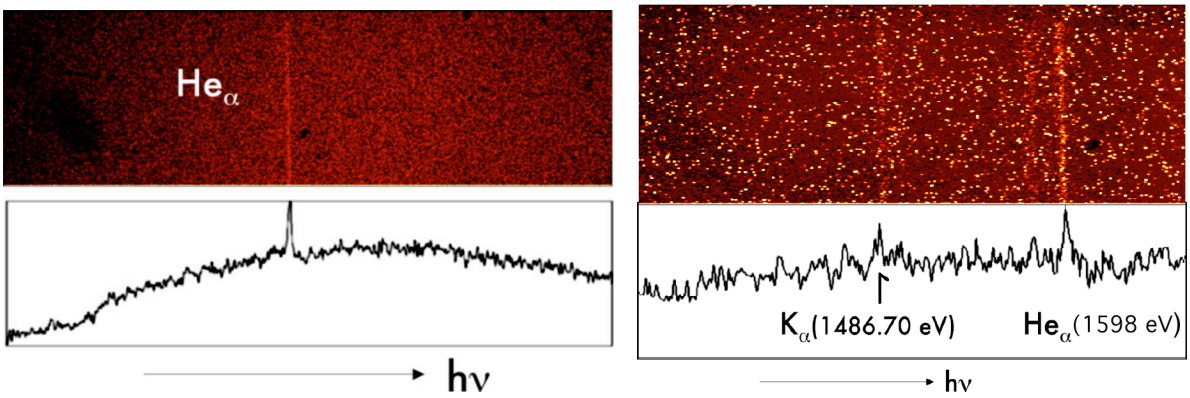

Figure 8. X-ray spectrum obtained from laser irradiation of a solid Al target using a flat TlAP crystal spectrometer with the same experimental setup except for the incident laser pulse parameters. The spectrum on the left was obtained from irradiation with a 100 mJ level, ns laser pulse focused at an intensity of 10^{12} W/cm^2. The spectrum on the right was obtained irradiating the target with a 10 mJ level pulse with a duration of a few ps, focused at an intensity close to 10^{16} W/cm^2.

Further insight in this issue can be gained taking direct, single photon events in a sufficient number to build up a statistically significant energy dependence upon the energy of a single event. In fact, it is now well established [16] that each event detected by the CCD can be analysed to retrieve the actual charge produced in the CCD pixels. This charge can then be converted into the incident X-ray photon, via independent energy calibration [16].

This technique was used to investigate the effect of a change of focused intensity due to change of CPA pulse duration in the sub-ps level. In this case, the change of pulse duration was achieved by changing the configuration of the final compressor of the TiSa laser system. The plot of Figure 9 (left) shows the single-event spectra obtained with 250 fs (black line) and 500 fs pulses (blue line) containing the same energy of approx. 10 mJ. Both spectra show a line emission the K-alpha Al line at 1486 eV partially merged with a low intensity He-alpha from He-like Al plasma at 1598 eV as shown in detail in the plot of Figure 9 (center). Both spectra showa rapidly decreasing high energy component. In the higher intensity case, this component extends up to 30 keV range with an additional peak just below 40 keV.

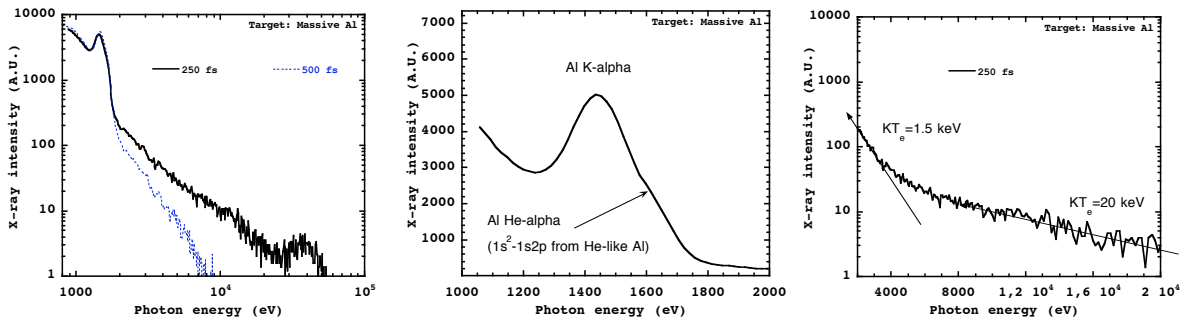

Figure 9. (left) Single photon spectra obtained from laser irradiation of a solid Al target irradiated by a 10 mJ laser pulse at two different values of the pulse duration, namely 250 fs (blach line) and 500 fs (blue line). (right) (center) Expanded plot of the line-emission component of the spectrum showing the main K-alpha line and the contribution of line emission from He-like al plasma. (right) Exponential fit of the higher energy portion of the 250 fs curve.

The rapidly decreasing part of the spectrum is shown in detail in Figure 9 (right). Also shown in the figure is the exponential fit for the lower and higher energy end of the plot. According to this fit, the higher energy end of the X-ray spectrum decreases exponentially with a constant of 20 keV. This parameter is linked to the energy distribution function of fast electrons. According to the model of fast electron generation [17], the fast electron energy is related to the $I\lambda^2$ parameter of the incident laser light according to the following relation:

$$T_{hot} = \left[\sqrt{\left(1 + \frac{I\lambda^2}{2.8 \times 10^{18}} \right)} - 1 \right] 511 \text{ (keV)}.$$

At the incident laser intensity of approximately 5×10^{16} W/cm^2 corresponding to the data plotted in Figure 9 (right), the fast electron temperature is expected to be in the 10 keV range, consistent with the observed values. A more detailed description of this mechanism is in progress.

3. The Ti-K-alpha source

According to the above model, the temperature of the fast electron population can be therefore further increased at higher laser irradiances. This is necessary when higher K-alpha X-ray energy is aimed for. In fact, it is planned to set up an X-ray source of sufficiently high photon energy to be employed in X-ray diffraction experiments. According to the above results on the electron distribution energy from Al target, we can reasonably expect that K-alpha emission up to the Cu-K-alpha (8 keV) should be accessible. At the present stage, we decided to set our working point at the K-alpha of Ti at 4.51 keV photon energy. This value ensures the possibility of achieving a sufficiently high photon flux and at a photon energy sufficiently short to enable X-ray diffraction studies with a wide range of materials.

The plot of Figure 10 shows K-alpha emission from a Ti target, irradiated with a 12 mJ pulses with a pulse length optimised at 67 fs (FWHM) as shown in the plot of Figure 4 (right). As expected, the main emission component due to the K-α line at 4.51 keV is clearly visible in the plot. Also visible in the plot is the so-called escape peak, due to energy loss of one Si K-alpha photon arising from interaction of primary photoelectrons generated by the incident Ti-K-alpha photons in the CCD pixels.

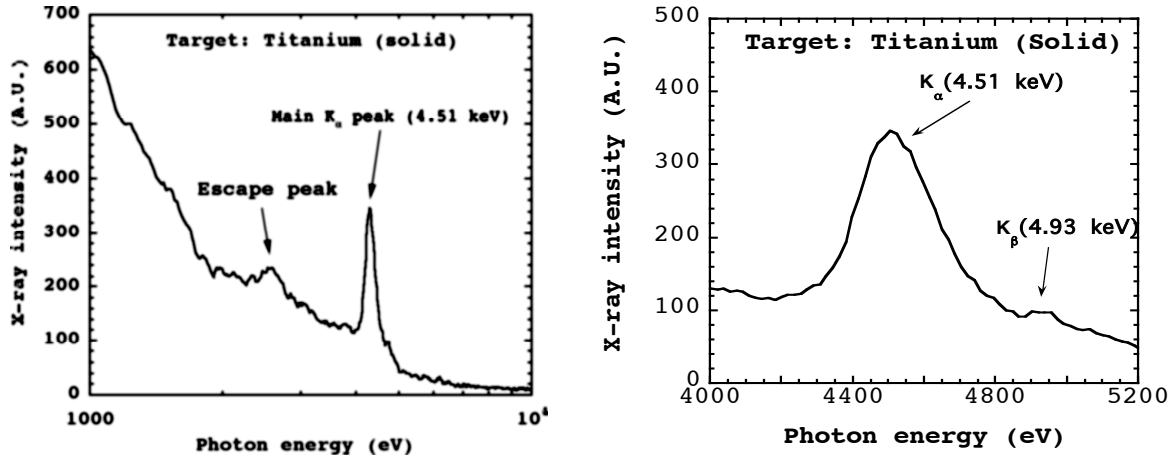

Figure 10. Spectrum of the X-ray emission produced during the irradiation of a solid Ti target by a 67 fs laser pulse at an intensity above 10^{16} W/cm^2. The main line visible in the spectrum is the Ti K_α line at 4.51 keV. Also visible on the low energy side of the Ti K-α line is the so-called escape peak due to loss of Si K- α photons in the CCD silicon active layer. The plot on the right shows that the K_β line at 4.93 keV is also visible.

The detection technique used to obtain the spectra of Figure 10 enabled us to obtain simultaneously the total flux of X-ray photons emitted by the source at the Ti- K-α photon energy. In fact, as discussed above, the CCD based technique used in our experiments enabled us

to measure the photons emitted by the source at every laser shot. Taking into account the solid angle of view of the CCD and assuming an isotropic distribution of emission, we find out that our X-ray source emits approximately 10^7 photons per pulse at 4.51 keV. Since the source can operate at a repetition rate of 10 Hz, that is the rep-rate of the driving laser pulse, we estimate an average X-ray power of 70 nW.

We point out here that the main attractiveness of this class of sources is the short duration of the X-ray pulses. In general, the X-ray pulse duration will be mainly determined by the driving laser pulse duration. However, several interaction parameters including the target geometry, will contribute to lengthening the pulse.

TARGET	PHOTON ENERGY	TOTAL FLUX	REP-RATE	DIVERGENCE	PULSE DURATION	SOURCE SIZE
Ti	4.51 keV	10^7 per pulse	10 Hz	Isotropic	<<1ps	$\approx 10\ \mu$m

Table 1. Summary of main parameters of the laser-driven, ultra-fast X-ray source running with the Ti target.

Although a direct measurement of our X-ray pulse duration has not been carried out yet, measurements performed in similar experimental conditions [18] show that in the case of 100 fs laser pulse, an X-ray pulse-length between 200 fs and 600 fs may be expected. It is reasonable to assume that in our set up, the X-ray pulse duration will be in the range of a few hundreds of femtoseconds. A summary of the main parameters of the X-ray source operating with the Ti target is shown in Table 1.

4. Conclusion

A description of the recent work carried out at the Intense Laser Irradiation Laboratory (IPCF-CNR) on the set-up and characterization of a laser-driven, ultrafast X-ray source has been given. The source is now operational and running with the performances given in Table 1. Future work includes extension to other X-ray photon energies (e.g. Cu k-alpha) and detailed characterization of temporal and spatial features of the source. Nonetheless, applications of the operational Ti source are foreseen within the frame of national and international collaborations.

[1] D.Giulietti and L.A.Gizzi, *X-ray emission from laser-produced plasmas*, La Rivista del Nuovo Cimento **21**, 1 (1998).

[2] D. Stickland and G. Mourou, *Compression of amplified chirped optical pulses*, Opt. Commun. **56**, 219 (1985).

[3] Rose-Petruck et al., *Picosecond-milliångström lattice dynamics measured by ultrafast X-ray diffraction* Christoph Nature, **398**, 310 - 312 (25 Mar 1999);

[4] A. Rousse, C. Rischel, J.-C. Gauthier, *Femtosecond X-ray crystallography*, *Rev. Modern Physics* **73**, 17 (2001).

[5] A.Rousse et al., *Non-thermal melting in semiconductors measured at femtosecond resolution*, Nature, **410**, 65 - 68 (01 Mar 2001);

[6] L.A.Gizzi, A.J.Mackinnon, D.Riley, S.M.Viana, O.Willi, *Measurements of thermal transport in plasmas produced by picosecond laser pulses,* Laser Part. Beams, **13** (1995) and references therein.

[7] D.Riley, L.A.Gizzi, A.MacKinnon, S.M.Viana, O.Willi, *Absorption of High Contrast 12 ps UV Laser Pulses by solid targets,* Phys. Rev. E, **48**, 4855 (1993).

[8] D. Salzmann, Ch. Reich, I. Ushmann, E. Forster, P. Gibbon, "Theory of Kalpha generation by femtosecond laser-produced hot electrons in thin foils", *Phys. Rev. E* **65**, 036402 (2002).

[9] Ch. Reich, I. Ushmann, P. Ewald, S. Dusterer, A. Lubcke, H. Schwoerer et al., "Spatial characteristics of kalpha X-ray emission from relativistic femtosecond laser plasmas", *Phys. Rev. E* **68**, 056408 (2003).

[10] Ch. Reich, P. Gibbon, I. Ushmann, E. Forster, "Yield optimization and time structure of femtosecond laser plasma Kalpha sources", *Phys. Rev. Lett.* **84**, 4846 (2000).
[11] D.Giulietti, L.A.Gizzi, A.Giulietti, A.Macchi, D.Teychenneé, P.Chessa, A.Rousse, G.Cheriaux, J.P.Chambaret, G.Darpentigny, *Observation of solid-density laminar plasma transparency to intense 30-femtosecond laser pulses*, Phys. Rev. Lett. **79**, 3194 (1997).
[12] L.A.Gizzi , D.Giulietti, A.Giulietti, T.Afshar-Rad, V.Biancalana, P.Chessa, E.Schifano, S.M.Viana, O.Willi, *Characterisation of Laser Plasmas for Interaction Studies*, Phys. Rev. E, **49,** 5628 (1994), erratum **50,** 4266 (1994).
[13] L. Labate, M. Galimberti, A. Giulietti, D. Giulietti, L.A. Gizzi, P. Köster, S. Laville, P. Tomassini, *Ray-tracing simulations of a bent crystal X-ray optics for imaging using laser-plasma X-ray sources,* Laser Part. Beams **22**, 253 (2004).
[14] S. A. Pikuz, T. A. Shelkovenko, V. M. Romanova, D. A. Hammer, A. Y. Faenov, V. A. Dyakin, and T. A. Pikuz, *Monochromatic x-ray probing of an ultradense plasma*, JETP Lett. **61,** 638–644 1995.
[15] L.A.Gizzi, D.Giulietti, A.Giulietti, P.Audebert, S.Bastiani, J.P.Geindre, A.Mysyrovicz, *Simultanoeus measurements of hard X-rays and 2nd harmonic emission in fs laser-target interactions,* Phys. Rev. Lett. **77**, 2278 (1996).
[16]L. Labate, M. Galimberti, A. Giulietti, D. Giulietti, L.A. Gizzi, P. Tomassini, G. Di Cocco, *A laser-plasma source for CCD calibration in the soft X-ray range,* Nucl. Instr. and Meth. A. **495**, 148 (2002).
[17] S.C. Wilks, W.L. Kruer, M.Tabak, A.B.Langdon, *Absorption of Ultraintense Laser Pulses*, Phys. Rev. Lett. **69**, 1383 (1992)
[18]T. Feurer, A. Morak, I. Uschmann, C. Ziener, H. Schwoerer, C Reich, P. Gibbon, E. Forster, R. Sauerbrey, K. Ortner, C.R. Becker, *Femtosecond silicon K alpha pulses from laser-produced plasmas*, Phys. Rev. E, **65**, 016412 (2001)